MARS EXPRESS HRSC ANALYSIS OF TWO IMPACT CRATERS IN TERRA TYRRHENA, MARS. J. Korteniemi[1], V.-P. Kostama[1], M. Aittola[1], T. Öhman[1,2], T. Törmänen[1], H. Lahtela[1], J. Raitala[1], G. Neukum[3] and the HRSC Science Co-Investigator team. [1]Astronomy, Department of Physical Sciences, University of Oulu, P.O. Box 3000, FIN-90014 Oulu, Finland <jarmo.korteniemi@oulu.fi>, [2]Department of Geosciences, University of Oulu, Finland, [3]Institute of Geosciences, Freie Universität Berlin, Germany

Introduction: The surface of Mars is governed by division to smooth northern lowlands and intensely cratered highland terrain in the south. The cratering record indicates the age of the surface [e.g. 1,2], while individual craters' original morphology hints to the target material at the time of impact [3]. Additionally, the craters provide natural sinks for later deposited materials, thus showing glimpses of the evolution of the region they reside in. In all, craters provide information on the local and areal evolution phases and processes.

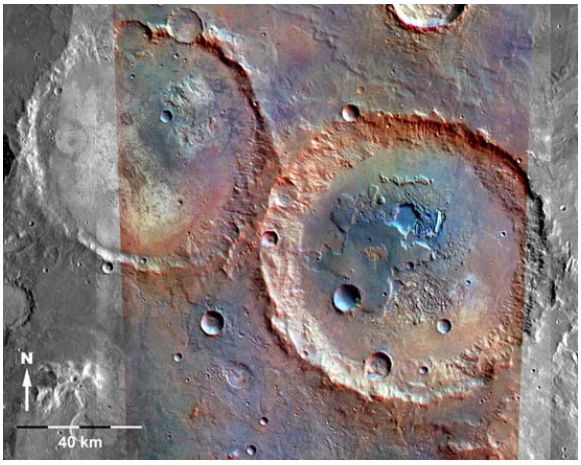

Figure 1. Mosaic of enhanced color HRSC RGB image and complementing THEMIS day-IR images showing the studied craters. The white star and arrow show the direction of sunlight.

Hellas impact basin dominates the southern hemisphere of Mars. Its complimentary region has volcanic, tectonic, glacial, fluvial and aeolian features [e.g. 4-9], as well as a multitude of large and small impact craters. Two of them, a pair of large, roughly same sized unnamed impact craters are located in Terra Tyrrhena, on the northeastern Hellas rim [10]. In this study, these are analyzed and interpreted using new Mars Express HRSC data, in order to explain their modification history. This also in part helps us to understand the changes in the environment, and furthermore the evolution of the region, most importantly Hellas basin interaction with its surroundings [e.g. 8]. Hereafter, the eastern crater (24.5°S 80.8°E) will be referred to as *crater A* and the western crater as *crater B* (23.9°S 79.3°E). This almost adjoined pair of craters (Fig. 1) harbors a complex morphology comprised of several material units with distinct topographies. The floors show varied features unlike in any other craters in the region, e.g. deep pits with intervening filament-like ridges, a peak ring, a large central massif of layered material and rugged, highly eroded terrain.

The studied craters: The floors of the studied craters show topographically and morphologically anomalous features compared to 'regular' impact craters [e.g. 3, 11]. The two craters are of different ages but show similarities in their floor features, indicating that most of them have been created by post-impact processes. The floor morphologies are complex, requiring a multitude of events and processes to explain them. In order to discover the evolution sequence, we first defined the geomorphologic units and looked at their individual characteristics. Each unit had a distinct topography level and extent where they occurred, hinting to the layered nature of the materials.

Crater A (the eastern crater, Fig. 1) is 95 km in diameter and in relatively pristine condition; the elevation difference between crater floor and surrounding plains is 1200m, and the almost intact rim towers on average 750 m above the plains. The crater has some ejecta blanked left in the north-western region. The inner walls are cut by mainly mass wasting furrows, but some more fluvial-like channels are also present, though they are much less prominent than on the walls of the Crater B. The crater floor is dominated by a central massif and a multitude of pits. After the main impact, ~680 smaller craters visible with in HRSC data have been formed on its floor. From these, we calculated size-frequency distribution curves for floor units. Due to the small areas (500-1500 km^2), only a few >1 km craters have accumulated on the units. This increases the error margins and makes age determination according to Tanaka [12] possible, but difficult.

Crater B (the western crater, Fig. 1) has a diameter of 75 km, and it appears to be the more modified and older of the two. It has shallow topography and a highly modified broken rim structure which is observable only in places; the floor - surrounding plains elevation difference is 500 m, rim-plains ~400 m. The inner walls of the crater are cut by numerous small channels. While some are made by mass wasting processes, others are dendritic in nature and extend well onto the crater floor. The largest channel (width ~1 km) cuts the rim in the NW. The eastern part of the crater's inner wall has undergone a major mass wasting episode after and perhaps caused by the more recent Crater A forming impact event. Some features on the floor resemble the wrinkle ridges outside the crater, having similar topography and N-S direction. They also apparently breach

the southern rim, indicating continuation from the Nh wrinkle ridges. However, they are so eroded that no clear distinction can be made.

Geology of the craters: The craters were formed on the highly modified Noachian highlands (Nm), which is cut by numerous wrinkle ridges and fluvial channels (Fig. 2). Probably due to suitable target material, crater A was formed with a peak-ring structure. After their creation the craters have been filled with three different deposit types: volatile-rich, erodable and more erosion-resistant materials, each with their own elevation level where they occur. The total sediment thickness is 1700 m for the eastern Crater A and 2400 m for the western crater B. The average thickness of the sediments which we can see having been eroded are 400 m and 300 m, respectively.

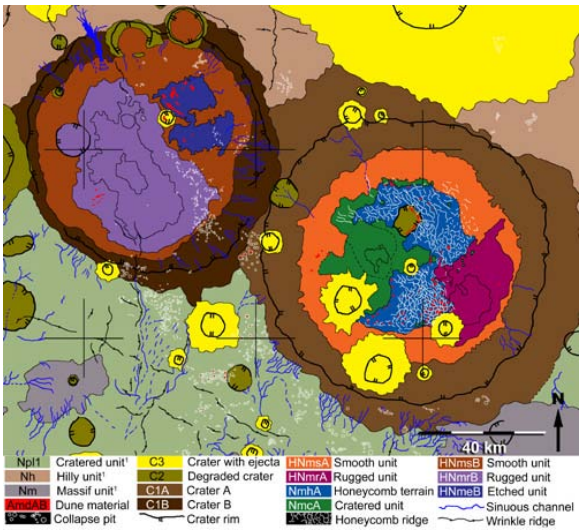

Figure 2. Geological map of the craters´ area showing the identified material and terrain units.

Crater A: The oldest observable sediments are the bright materials seen on the polygonal crater walls and on the floors of the pits. The same or similar bright material also occupies the base of the central massif. Later sedimentation included or retained more volatiles, which gathered inside the peak ring, and later froze or dried out, creating polygonal fractures. This resulted in intrusions of more durable and hard-wearing materials from the following sedimentation process, occupying the fractures and cementing in place. Several layers of materials superposed the unit, creating the material for the now-rugged unit $HNmr_A$ as well as creating the unit Nmc_A on the top of the massif. Subsequently the materials were eroded, dissecting the central massif. Creating first the rugged terrain to the east, erosion continued and digging deeper in the central areas it exhumed the erosion-resistant material ridges seen as polygonal features in Nmh_A. Then sedimentation of the smooth unit $HNms_A$ was followed by the emplacement of the Amd_{AB} dunes. Regional Hellas-related zones of weakness stresses affected the erosion throughout the evolution history, creating tensions also inside the crater which in the end resulted in the deep deformation and endogenic dike injections into the honeycomb terrain.

Crater B: This crater was more straight-forward in its evolution (Fig. 2); it was dominated by overlapping periods of compression, sedimentation and erosion. Some regional compression fields have still been active during the early sedimentation process, causing remnant wrinkle ridges we see on the floor. The underlying rugged sub-unit $HNmr_{B2}$ was superposed by another ($HNmr_{B1}$), and that in turn by the smoother and fluvially modified $HNms_B$ unit. Later erosion has dug deep (~150 m) into the central areas of the crater, revealing all three layers. A second center of erosion is the etched unit $HNme_B$, created into the smooth material. The etched material has also acted as a later sink for late fluvial and aeolian deposits.

Conclusions: The evolution of the craters (Fig. 1) has been dominated by sedimentation and erosion. The existence of a peak ring in the eastern crater (A) resulted in the capture of volatiles, and the creation of a very unusual landform, the honeycomb terrain. The erosion process was dominated by zones of weakness created by the southern Hellas basin. As similar collapse and erosion features inside craters are found mostly only in the vicinity of the Hellas basin, this raises a question on the nature of the special circumstances occurring in the region. The usage of the unprecedented MEX HRSC data with other existing and future data sets improves the possibilities in analyzing different landforms on Mars, and identifying their origins.

Acknowledgements: We thank Drs. A. Basilevsky, M. Kreslavsky and M. Ivanov for innovative discussions, new ideas and constructive criticism. We also gratefully acknowledge the efforts made by the MEX-HRSC Photogrammetry Team in processing the digital image data and the NRPIF for the use of working facilities.

References: [1] Kreiter, T.J. 1960, *Publications astronomical society of the Pacific*, 72, 393; [2] Hartmann, W.K. & G. Neukum 2001, *SSR*, 96, 165; [3] Melosh, H.J. 1989, *Impact Cratering*, Oxford Univ. Press, N.Y.; [4] Carr, M.H. & G.G. Schaber 1977, *JGR*, 82, 4039; [5] Crown, D.A. et al. 1992, *Icarus*, 100, 1; [6] Crown, D.A. & R. Greeley 1993, *JGR*, 98, 3431; [7] Leonard, G.J. & K.L. Tanaka, 2001, *USGS Map I-2694*; [8] Raitala et al., 2004; [9] Öhman et al. 2005, in: *Impact Tectonism, Henkel H. & Koeberl C., eds., Springer,* Berlin-Heidelberg, in press; [10] Tanaka, K.L. & G.J. Leonard, 1995; [11] Strom, R.G. et al. 1992, in: *Mars, H.H. Kieffer, B.M. Jakosky et al., eds.,* Univ. of Arizona Press, Tucson, 383; [12] Tanaka, K.L. 1986, *JGR*, 91, 139.